Anal. Bioanal. Electrochem., Vol. 17, No. 4, 2025, 273-283
https://www.doi.org/10.22034/abec.2025.723270

Analytical & Bioanalytical Electrochemistry

Full Paper

Octylamine Assisted Hydrothermal Growth of Silver Sulphide Nanoparticles as Efficient Electrode Material for Energy Storage Application

Sanghamitra Mohapatra, Tapan Kumar Sarangi, Rashmita Panda, and Kusha Kumar Naik*

P.G. Department of Physics, Berhampur University, Odisha, Pin:760007, India

*Corresponding Author,
E-Mail: kkn.phy@buodisha.edu.in

Received: 23 January 2025 / Received in revised form: 3 April 2025 / Accepted: 22 April 2025 / Published online: 30 April 2025

Abstract- This study systematically investigates the electrochemical energy storage performance of hydrothermally synthesized silver sulfide (Ag_2S) nanoparticles as an advanced electrode material for supercapacitors. Structural, morphological, and optical analyses were conducted using X-ray diffraction (XRD), scanning electron microscopy (SEM), and UV-visible spectroscopy, confirming the successful synthesis and phase purity of Ag_2S nanoparticles. The electrochemical properties were evaluated in a three-electrode system using Na_2SO_4 electrolyte through cyclic voltammetry (CV), galvanostatic charge-discharge (GCD), and electrochemical impedance spectroscopy (EIS). The Ag_2S electrode exhibited a remarkable specific capacitance of 562.5 F/g, a high energy density of 145.8 Wh/kg, and a power density of 84 W/kg, demonstrating strong pseudocapacitive behavior with efficient charge storage capability. Furthermore, the electrode displayed excellent cyclic stability, retaining 90% of its initial capacitance even after 5000 charge-discharge cycles. These results highlight the immense potential of Ag_2S nanoparticles as a high-performance electrode material, contributing to the advancement of next-generation energy storage devices.

Keywords- Octylamine; Silver Sulphide; Nanoparticles; Supercapacitance; Hydrothermal

1. INTRODUCTION

Nowadays, research has been focused on renewable energy and energy storage devices with the highest performance and efficiency without harming the ecosystem [1-3], Although energy storage devices such as batteries, fuel cells, and capacitors are paving the way for power demands with appropriate performance and stability, much more energy is needed to satisfy the current energy demands for different electronics applications [4]. So, a suitable device and novel technology are required that shall fulfill the energy requirements while minimizing the environmental consequences. Many modern devices need instant, quick, and high magnitudes of energy for their performance, that can be produced through controlled chemical reactions that are clean and renewable [5,6]. Compared to conventional energy storage devices like batteries, fuel cells, and capacitors, supercapacitors deal with electrochemical reactions but offer high energy density and greater power density in a short span of time with quick cycles of charge and discharge [7-10]. The performance of a supercapacitor could be enhanced manyfold by engineering the physicochemical characteristics of a supercapacitor, such as its elemental composition, surface structure, structural geometry, electrical conductivity, chemical reaction, etc. [11,12]. So, a suitable nanomaterial is required that is physically stable and chemically more reactive to perform robust material properties.

Sulphide has been used extensively as an active electrode material due to its unique conductivity and arrangement with the metal ions, which promotes faster carrier movement and electrochemical reactions on the electrode surface [13]. Therefore, many reports have been made for a variety of metal sulphides like aluminum, iron, vanadium, molybdenum, tungsten, lanthanum, cobalt, copper, nickel, and zinc, etc. [14-17]. Peng et al. synthesized the TP-Ni_xS_y/rGO hybrid structure electrode material in a simple process for the use of an energy storage device, and the high energy and power density of the electrode material were demonstrated [18]. Gupta et al. constructed the 2D-layered structure and high surface area of MoS_2 by hydrothermal method and used it as electrode material for supercapacitors to achieve high energy density and capacitance retention [19]. Arulraj synthesized Ag_2S nanomaterial on Ni mesh , as binder free electrode material which shows great specific capacitance [20]. Rabia synthesized Ag2S-Ag2O-Ag nano composite as promising two electrode symmetric supercapacitor electrode material which tested in both acidic and basic medium showed superior capacitance [21]. Similarily, Abbas synthesized hydrothermally highly efficient AgSrS electrode material which showed significant supercapacitance [22]. Silver is well known for its conductivity, reactivity, and catalytic nature. So, silver could be bonded with sulphur by the hydrothermal method for the formation of silver sulphide, and high material properties could be expected from silver sulphide due to its unique electrochemical and structural properties. It exhibits moderate electrical conductivity with tunable semiconducting behavior, which enhances charge transport and storage efficiency. Ag_2S also demonstrates excellent electrochemical stability, ensuring long-term performance with minimal degradation

over multiple charge-discharge cycles. Its redox-active nature enables reversible faradaic reactions, contributing to enhanced pseudocapacitive behavior and higher energy storage capacity. Additionally, Ag_2S nanoparticles offer a high surface area, facilitating rapid ion diffusion and improving charge storage efficiency [23,24].

Usually, chalcogenide materials are used to prefer a vacuum state for their nucleation and growth of the particles. In this work, we have reported the simple and cheap synthesis of Ag_2S nanomaterials with a monoclinic lattice by the economical hydrothermal approach employing octylamine as the synthesis medium. Scanning electron microscopy (SEM), X-ray diffraction (XRD), and UV-visible spectroscopy are employed to confirm the structural, morphological, and optical aspects of the Ag_2S material. Finally, the electrochemical properties of the Ag_2S nanoparticles are revealed to have a specific capacitance of 562.5 F/g at a scan rate of 2 mV/s from cyclic voltammetry (CV) and 525 F/g at a current density of 70 A/g from Galvanostatic charge discharge (GCD), with good charge and discharge durability using a three-electrode electrochemical setup configuration.

2. EXPERIMENTAL SECTION

2.1. Material Synthesis

The simple and cheap hydrothermal approach was used to produce silver sulphide nanoparticles, taking $AgNO_3$ (silver nitrate), S (sulphide powder) as precursors and octylamine as solvent because it acts as a capping agent to prevent agglomeration and control morphology, also can mildly reduce Ag^+ ions. Additionally, its hydrophobic nature enhances nanoparticle dispersibility in organic solvents. At first, 0.2717 g (80 mM) of $AgNO_3$ and 0.0256 g (40 mM) of sulphur powder were dissolved in 10 ml of octylamine in separate beakers and stirred for 20 minutes for proper dispersion. After that, both solutions were mixed and transferred to a 25-ml autoclave for heat treatment at 423 K for 16 hours.

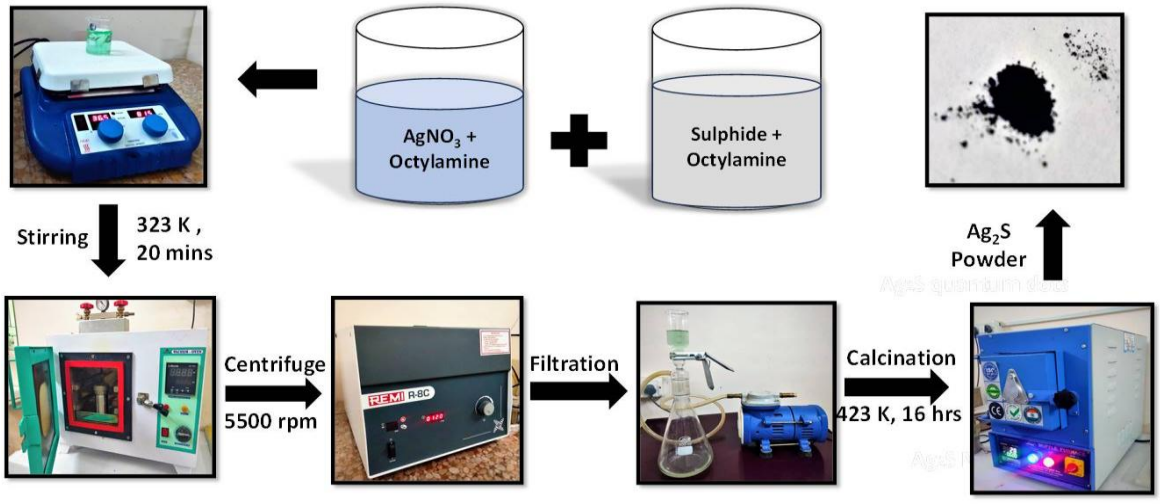

Figure 1. Schematic representation of the synthesis process of the Ag_2S nanoparticles

At the high temperature, the dissolved "Ag and S" ions reacted with themselves through oxidation and reduction by gaining thermal energy and leading to the nucleation, growth, and phase transformation of Ag_2S molecules. Further, Ag_2S molecules aggregated with one another under intramolecular force governed by synthesis parameters for the growth of Ag_2S nanoparticles. Finally, the precipitated solution was washed and cleaned several times by ethanol to get the pure Ag_2S nanoparticles and dried at room temperature for different experimental studies. Figure 1 shows the synthesis process of the produced Ag_2S nanoparticles for better knowledge and visualization.

2.2. Material Characterization

The crystal structure and crystallite size of the as-synthesized material were ascertained using an X-ray diffractometer (PROTO AXRD, Cu-Kα radiation, λ = 1.54 Å), and the morphology was investigated under a SEM (Flex-SEM 1000). A UV-visible spectrophotometer (Labtronics, Model LT-2 201) was used to determine the emission spectra of the Ag_2S nanoparticles from which the band gap of the nanomaterial can be determined.

2.3. Electrochemical measurement

The electrochemical performance of Ag_2S nanoparticles was investigated executing a Potentiostat (Sinsil International LTD) instrument in a three-electrode configuration set up taking 1 M of Na_2SO_4 as an electrolyte. Because, Na_2SO_4 have neutral pH, which ensures material stability, prevents unwanted side reactions, and enhances cycling life and It offers high ionic conductivity and low charge transfer resistance, improving charge storage efficiency. Additionally, it is non-corrosive, environmentally friendly, and electrochemically stable, making it a safe and effective choice for energy storage application. The synthesized silver sulphide coated in a glassy carbon electrode was used as the working electrode, followed by platinum wire as the counter electrode and a saturated calomel electrode as the reference electrode, respectively. To find the redox potential of the Ag_2S nanoparticle, the CV experiment was carried out in a potential window spanning from -1V to 1V with different scan rates, and the GCD test was executed in the same potential range but in different current densities. Similarly, an electrochemical impedance spectroscopy (EIS) experiment was carried out in the frequency range from 10 kHz to 0.01 Hz to investigate the electrochemical performance of the synthesized nanomaterial. The specific capacitance of silver chalcogenide nanoparticles was computed employing equations (1) and (2), which are given below.

$$Cs = \frac{1}{2\times m\times v\times \Delta V}\int_{Va}^{Vb} i(v)dV \quad (1)$$

$$Cs = \frac{i\times \Delta t}{m\times \Delta V} \quad (2)$$

Where ‘i’ is the current in (A),'m’ is the mass of the electrode material in (0.1 mg), ‘Δt’ is the discharge time in (s), scan rate is in (mV/s), and potential window is in (V).

3. RESULTS AND DISCUSSION

3.1. Structural investigation

An X-ray diffractometer was used to determine the structural analysis of Ag_2S nanoparticles, and its XRD pattern is supplied in Figure 2(a). The characteristic peaks obtained at different angles (2 theta) are distinct, distinguishable, sharp, and assigned to the miller indices of (-102), (-012), (-110), (-113), (-121), (-122), (-120), (-104), (-031), (-202), (-121), (-214), (-014), (-215), (-142), (-233), (-106), and (-135), respectively. All of the observed peaks acquired at various angles are attributed to the Ag_2S material, and the high-pitched characteristic peaks of the Ag_2S showed crystallinity (JCPDS card 01-075-1061). There are no other peaks of Ag_2S nanoparticles identified, indicating that the generated material is pure in nature.

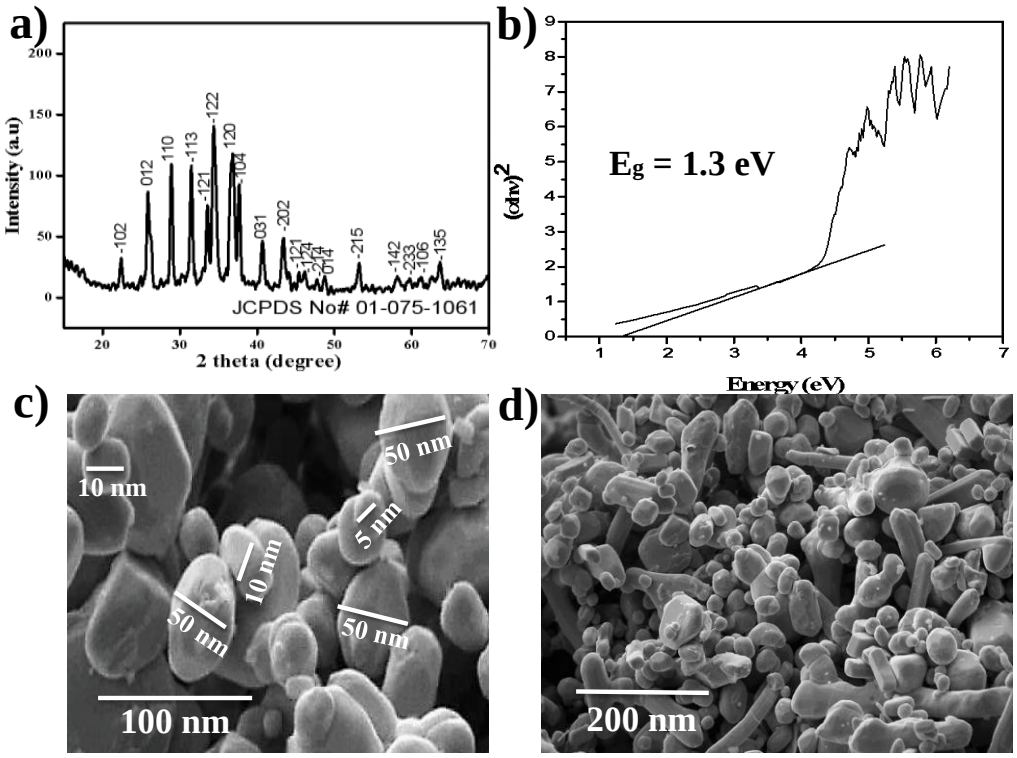

Figure 2. (a) XRD pattern of Ag_2S material; (b) Band gap of Ag_2S material; (c) Magnified SEM image of Ag_2S nanoparticles; (d) SEM image of Ag_2S nanoparticles

Similarly, Figure 2(b) illustrates the band gap of the produced Ag_2S nanoparticles to be 1.3 eV, which is semiconducting in nature. The semiconducting nature of the synthesized nanoparticles would enable greater charge storage kinetics and supercapacitive performance.

The SEM was employed to determine the morphological feature of the Ag_2S material, as illustrated in Figures 2(c-d),These images confirm the successful synthesis of Ag_2S spheroidal nanoparticles with a size range of 5 nm to 50 nm.The transformation from spherical to spheroidal morphology in Ag_2S nanoparticles is driven by anisotropic growth kinetics, reaction conditions, precursor effects, and surface interactions.It is expected that the nanoparticles would contain huge specific surface area, electron confinement, a short electron transport channel, and simple surface functionalization mechanics, which are advantageous for supercapacitor applications.

3.2. Electrochemical investigation

The CV and GCD experiments were conducted in three electrode configurations set up, taking 1 M of Na_2SO_4 as electrolytic solution. The CV of the Ag_2S nanoparticle electrode material was executed at various san rates to identify the oxidation and reduction potential of the nanomaterial. The oxidation peak obtained at 0.45 V and reduction peak at -0.5 V are assigned to Ag_2S nanoparticles, as shown in Figure 3(a). The redox peaks are distinct and homogenous in nature, signifying consistent electrocatalytic behavior of the produced Ag_2S nanoparticles. The redox behavior of the Ag_2S nanoparticles is clearly indicating the pseudocapacitive nature of the energy storage devices.

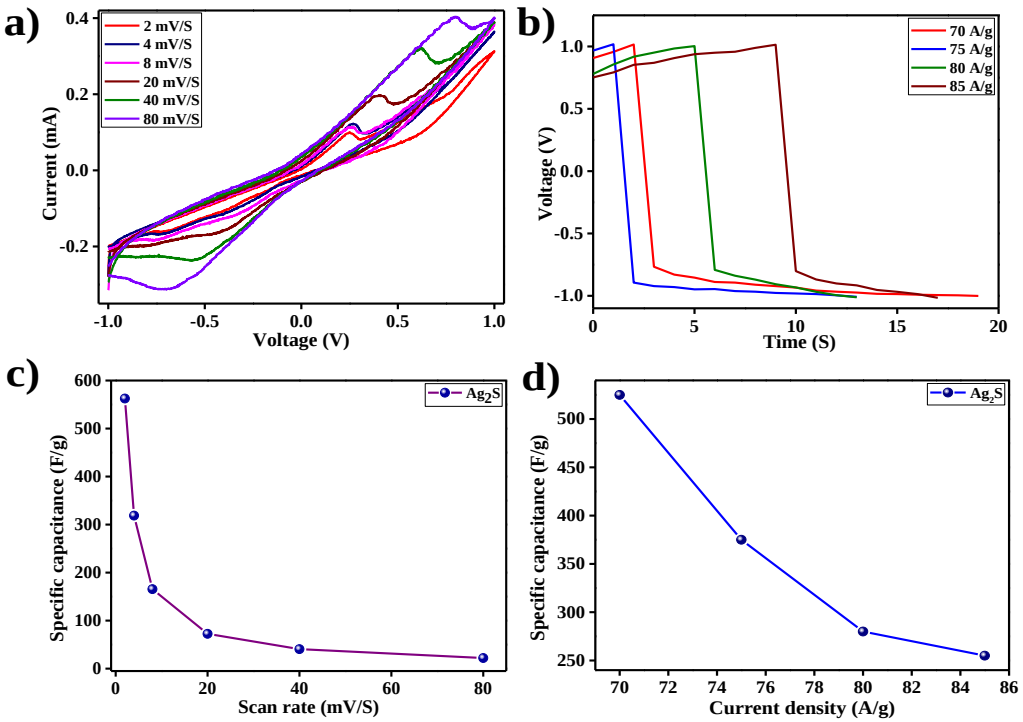

Figure 3. (a) CV curves of Ag_2S nanoparticles at different scan rates; (b) GCD curves of Ag_2S nanoparticles at different current densities; (c) specific capacitance performance of the synthesized nanoparticles with various scan rates; (d) Plot between specific capacitances with various current densities

The current intensity of CV rises effectively with increasing scan rate; as a result, the area bounded by closed curves increases eventually. In low scan rates, the ions available in the electrolyte solution have greater time to adsorbed on the Ag_2S nanoparticles surface and higher charge storage will be possible. Similarlly, the large storage capacity and supercapacitive performance of the Ag_2S nanoparticles would be due to increased active ion interaction with the active molecules of the nanoparticles, lower double layer and polarisation effects. The shifting of redox peaks in CV attributed to several factors i.e at higher scan rates, Ion diffusion and interaction played a crucial role, as Na^+ and SO_4^{2-} ions interact with the Ag_2S electrode surface, affecting charge storage mechanisms and causing diffusion limitations.

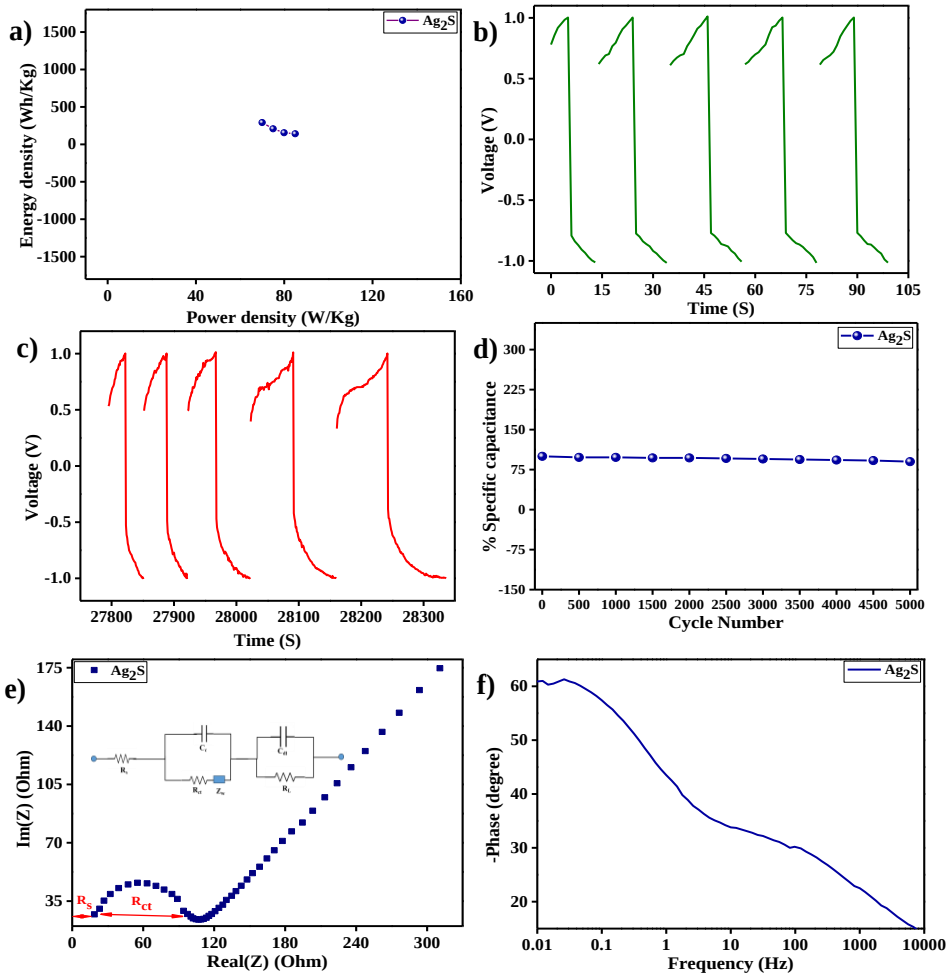

Figure 4. (a) Plot between Power Density with Energy density; (b) Charge and discharge time of Ag_2S of first five cycles; (c) Charge and discharge time of Ag_2S of last five cycles; (d) Plot between specific capacitances with various cycle numbers; (e) Nyquist plot of Ag_2S; (f) Bode plot of Ag_2S at frequency range 0.01 Hz to 10 kHz

The electrochemical reaction kinetics of Ag_2S, involved reversible oxidation and reduction of Ag and S species, also contributed to peak shifts due to variations in charge transfer

resistance and passivation layer formation. Structural stability is another factor, as repeated redox cycling induced phase transformations, strain effects, and even amorphization, leading to irreversible shifts in peak potential.

The GCD curve of Ag_2S nanoparticles has been plotted at different current densities, and its result is depicted in Figure 3(b), which demonstrated the charging and discharging capabilities of the Ag_2S nanoparticles. The charge and discharging times of the Ag_2S nanoparticles are calculated to be 2 and 12 seconds, which is suitable for supercapacitor applications. Figure 3(d) specifies the relationship between the specific capacitance and current charge density of the Ag_2S nanoparticles, which demonstrated the current density increases eventually as the specific capacitance falls. The real reasons behind this may be due to reduction or oxidation of active species at the electrode-electrolyte interface, effective surface area available for charge storage, ion migration, concentration polarization, and electrical resistance of the Ag_2S nanoparticles.

Similarly, Figure 4(a) provides the energy density and power density graph of the Ag_2S nanoparticles, which is 145.8 Wh/kg, and 84 W/kg respectively which is remarkable for supercapacitor application. High power density symbolizes quick charging and discharging, which is beneficial for rapid energy transfer and backup power systems in electronic equipment. The high power density and moderate energy density mean longer lifespan than batteries and greatest advantages for supercapacitor application. Figure 4(b) and (c) demonstrate the initial and final five cycles of charging and discharging of the Ag_2S nanoparticles, which is almost the same of charging and discharging times performance. The 1000-cycle GCD experiment was conducted to verify the stability in electrochemical performance of the produced Ag_2S nanoparticles, and approximately the same charging and discharging characteristics were noted as shown in Figure 4(d). As a result, an impressive 90% preservation of supercapacitance performance even after 5000 cycles was recorded.

Table 1. Comparison table of specific capacitances of Ag_2S nanospheroids with other sulphide materials

Composition	**Techniques**	**Specific capacitance (F/g)**	**Reference**
Ni–ZnS	Magnetron co-sputtering	134	[18]
Ni_3S_2@MoS_2	One step solution	425	[25]
MoS_2@MnS	Metal phase	410.4	[26]
MoS_2	Diffusion	357	[19]
Ag2S-Ag2O-Ag	Photo Polymerisation	92.5	[21]
Ag_2S -Ni	Chemical bath deposition	179	[20]
AgSrS	Hydrothermal	494.5	[22]
Ag_2S	Hydrothermal	562.5	**present work**

To find the frequency response of Ag_2S nanoparticles, EIS was conducted at open circuit potential over a frequency range of 10 kHz to 0.01 Hz. The frequency response of the Ag_2S electrode material is displayed in the Nyquist plot in Figure 4(e). The presence of a slanting line at low frequency in the impedance spectra indicates that the Ag_2S electrode material is capacitive and has a rapid rate of ion diffusion. According to the magnified view of this plot, a semicircle is also investigated at the high frequency region, indicating a restriction in charge transfer (R_{ct}), which is 70 ohm, and at the electrode-electrolyte interface with a surface resistance (R_s) of 10 ohm.

The Bode plot of Ag_2S electrode material in Figure 4(f) reveals a phase angle of -62 degrees, confirming the electrode material's capacitive nature. Excellent specific capacitance is noted when the energy storage capacitance of the produced Ag_2S nanoparticles is compared to comparable transition sulphide materials found in the literature, as indicated in Table 1.

4. CONCLUSION

The Ag_2S nanoparticles were successfully synthesized using a cost-effective hydrothermal process and characterized through XRD, SEM, and UV-vis spectroscopy. Their electrochemical performance exhibited a high specific capacitance of 525 F/g at a current density of 70 A/g and 562.5 F/g at a scan rate of 2 mV/s, demonstrating their potential for supercapacitor applications. Notably, the Ag_2S nanoparticles delivered an impressive energy density of 145.8 Wh/kg and a power density of 84 W/kg, highlighting their effectiveness in energy storage. Moreover, they retained 90% of their initial capacitance even after 5000 charge-discharge cycles, indicating excellent long-term stability. Overall, these results suggest that Ag_2S nanoparticles offer a promising balance between energy and power density, making them suitable for high-durability, fast-charging supercapacitors with compact energy storage capabilities.

Acknowledgments

This work is supported by the OURIIP (OURIIP-21SF/PH/67) project sponsored by OSHEC, Govt. of Odisha, and the SERB (EEQ/2022/000147) project, Department of Science and Technology, Govt. of India. All the experimental work was carried out at the P.G. Dept. of Physics and Center of Excellence (CoE) of Berhampur University.

Declarations of interest

The authors declare no conflict of interest in this reported work.

REFERENCES

[1] N. De Nevers, Air pollution control engineering, Waveland Press (2010).

[2] M. Jaccard, Sustainable fossil fuels: the unusual suspect in the quest for clean and enduring energy. Cambridge University Press (2006).
[3] D.J. Soeder, and D.J. Soeder, "Fossil fuels and climate change," Fracking and the Environment: A scientific assessment of the environmental risks from hydraulic fracturing and fossil fuels (2021) pp. 155–185.
[4] P. Yang, and W. Mai, Nano Energy 8 (2014) 274.
[5] S. Glasstone, An introduction to Electrochemistry, Read Books Ltd. (2011).
[6] C.G. Zoski, Handbook of electrochemistry, Elsevier (2007).
[7] S.S. Karade, A. Agarwal, B. Pandit, R.V. Motghare, S.A. Pande, and B.R. Sankapal, J. Colloid Interface Sci. 535 (2019) 169.
[8] S. S. Karade, and B.R. Sankapal, J. Electroanal. Chem. 802 (2017) 131.
[9] C.D. Jadhav, S.S. Karade, B.R. Sankapal, G.P. Patil, and P.G. Chavan, Chem. Phys. Lett. 723 (2019) 146.
[10] J. Theerthagiri, and et al., Nanomaterials, 8 (2018) 256.
[11] R. Boddula, A. Khan, A. M. Asiri, and A. E. Kolosov, Handbook of Supercapacitor Materials. Wiley Online Library (2022.)
[12] K. K. Kar, Handbook of nanocomposite supercapacitor materials II, vol. 302. Springer (2020).
[13] R. Kumar, R. Matsuo, K. Kishida, M. M. Abdel-Galeil, Y. Suda, and A. Matsuda, Electrochim. Acta 303 (2019) 246.
[14] J. Gou, S. Xie, Y. Li, X. Kong, and C. Li, J. Mater. Sci.: Materials in Electronics 30 (2019) 15429.
[15] H. Wang, et al., Current Applied Physics 35 (2022) 7.
[16] M.W. Raza, et al., J. Nanoparticle Res. 23 (2021) 1.
[17] M.F. Iqbal, M.N. Ashiq, and M. Zhang, Energy Technology 9 (2021) 2000987.
[18] S. Peng, L. Li, H. Bin Wu, S. Madhavi, and X. W. Lou, Adv. Energy Mater. 5 (2015) 1401172.
[19] X. Wu, X. Xie, H. Zhang, and K.-J. Huang, J. Colloid Interface Sci. 595 (2021) 43.
[20] A. Arulraj, N. Ilayaraja, V. Rajeshkumar, and M. Ramesh, Sci. Rep. 9 (2019) 10108.
[21] M. Rabia, A. M. Elsayed, M. Abdallah Alnuwaiser, and A. A. A. Abdelazeez, Micromachines (Basel) 14 (2023) 1423.
[22] T. Abbas, M.W. Iqbal, S. Gouadria, et al. J. Solid State Electrochem. 27 (2023) 873.
[23] C. Ji, Y. Zhang, T. Zhang, W. Liu, X. Zhang, H. Shen, Y. Wang, W. Gao, Y. Wang, J. Zhao, and W.W. Yu, Journal of Physical Chemistry C 119 (2015) 13841.
[24] H. Mołnås, S.J. Paul, M.R. Scimeca, N. Mattu, J. Zuo, N. Parashar, L. Li, E. Riedo, and A. Sahu, Cryst. Growth Des. 24 (2024) 2821.
[25] J. Wang, D. Chao, J. Liu, L. Li, L. Lai, J. Lin, and Z. Shen, Nano Energy 7 (2014) 151.

[26] L. Wang, X. Tan, Q. Zhu, Z. Dong, X. Wu, K. Huang, and J. Xu, J. Power Sources 518 (2022) 230747.